Disclaimer of Variability Between Institutions.

†Indicates experiments done at Stanford University. Anesthesia supplement for in vivo experiments was pure oxygen, resulting in lower baseline uptake for all radiotracers.

‡Indicates experiments done at MSK. Anesthesia supplement for in vivo experiments was medical air, resulting in slightly hypoxic conditions and higher baseline uptake for all radiotracers.

†‡Indicates experiments done at both Stanford and MSK, with average data pooled.

In the spirit of full transparency, we have included all data done at Stanford and MSK and indicate where the data was collected to make our multi-institutional collaboration extremely clear for the reader. We have included thorough statistical analysis of not only vehicle vs. LPS groups for both pHLIC and control radiotracers, but also uptake of the pHLIC vs. control radiotracer between LPS groups. The key result highlighting the difference between LPS groups is represented in the ex vivo biodistribution at 24 h (Supplemental Fig. 18 and Supplemental Table 8), coupled to the autoradiography (Fig. 6) at 24 h and serves as an appropriate demonstration of specificity for the acid-sensitive radiotracer [^{64}Cu]Cu-NO2A-c[E_4W_5C]. We show significantly higher uptake with our pHLIC radiotracer in the brain compared to our [^{64}Cu]Cu-NO2A-c[R_4W_5C] control. Additionally, our biophysical measurements (Supplemental Fig. 6) indicate the pH-sensitivity of the pHLIC (^{nat}Cu-NO2A-c[E_4W_5C] vs. non-acid-sensitive control (^{nat}Cu-NO2A-c[R_4W_5C]), further supporting the specificity of our pHLIC tracer for acidosis. We hope the discrepancy in baseline uptake of tracer between institutions (albeit similar trends and statistics between vehicle and LPS groups) will serve as a reminder to the nuclear medicine field how anesthesia and oxygen content can significantly change radiotracer uptake, especially with radiotracers that cross the BBB. We hold ourselves and the rest of the community to the highest standards and demonstrate the need for rigor and reproducibility among multi-institutional collaborations.

*See references 2-6 for how oxygen and anesthesia time can affect cerebral blood flow and radiotracer uptake, particularly in neuroimaging.

Materials and Methods.

Synthesis and purification of pHLIC-NO2A Constructs. Cyclic peptides c[E_4W_5C] or c[R_4W_5C] (1 mg, 0.6-0.65 μmol) was mixed with 2× stoichiometric excess NO2A-maleimide (1.2-1.3 μmol) in a 90:10 mixture of anhydrous dimethylformamide (DMF):degassed phosphate-buffered saline (PBS) for 2 h at 37 °C. The conjugate was purified using C_{18} Preparative-HPLC with a 5-95% acetonitrile with 0.1% TFA over 40 min gradient (t_R = 25 min) and evaluated using matrix assisted light desorption-ionization time-of-flight mass spectrometry (MALDI-ToF) or liquid chromatography mass spectrometry (LCMS). Two additional peptides (another cyclic "pHLIC" variant and one linear "pHLIP") were also conjugated to NO2A-maleimide using similar methods.

Cold labeling of c[E_4W_5C] and c[R_4W_5C]. pHLIC-NO2A conjugates (20 μL, 16 nmol) was diluted in 0.1 M NH_4Ac (pH 5.5) and incubated with a 2× stoichiometric excess of $^{nat}CuCl_2$ at 80 °C for 15 min. ^{nat}Cu-c[E_4W_5C] ^{nat}Cu-c[R_4W_5C] were purified using a C_{18} Sep Pak with fractionated elutions of 100% ethanol. Fractions were validated for successful labeling and purity via LCMS, then pooled and lyophilized and sent to URI for biophysical measurements.

Biophysical Studies.

Liposome Preparation. Large unilamellar vesicles (LUVs) were prepared by extrusion. POPC (1-palmitoyl-2-oleoyl-sn-glycero-3-phosphocholine, Avanti Polar Lipids) were dissolved in chloroform, desolvated on a rotary evaporator, and left under high vacuum for several hours. The phospholipid film was then rehydrated in 10 mM phosphate buffer pH 8.0, the lipid bilayer was gently dissolved, and extruded 21 times through the membranes with 50 nm pore sizes to obtain LUVs.

***Steady-State Fluorescence*.** Freshly prepared peptides and POPC vesicles were mixed to have 3 μM of a peptide and 0.6 mM of lipids in the final solution. Steady-state fluorescence measurements were carried out on a PC1 spectrofluorometer (ISS, Inc.) under temperature control at 25 °C. Fluorescence was excited at 280 nm and recorded with the excitation and emission slits set at 4 nm. The polarizers

in the excitation and emission paths were set at the “magic” angle (54.7° from the vertical orientation) and vertically (0°), respectively.

***pH-Dependence*.** pH-dependent partitioning of the constructs into a lipid bilayer of the membrane was examined by the shift of the position of the fluorescence spectral maximum for the constructs in the presence of POPC liposomes induced by a drop of pH from 7.4 to 4 by the addition of HCl. The constructs were incubated overnight with 50-nm POPC liposomes (final concentration of the peptides and POPC in solution was 3 μM and 0.6 mM, respectively), and pH decrease was achieved by the addition of aliquots of 0.5 and 0.1 M HCl. pH was measured by micro-electrode probe (Thermo Electron Corporation, Orion Ross Micro pH electrode). Fluorescence spectra were recorded at each pH value. The spectra were analyzed by the decomposition algorithms using Protein Fluorescence and Structural Toolkit (PFAST) toolkit to establish the position of the emission maximum (*1*). Finally, the positions of the fluorescence spectral maxima (λ_{max}) were plotted versus pH, and the Henderson–Hasselbalch equation was used to fit the data (using Origin 9.0 software):

$$\lambda_{max} = \lambda_1 + \frac{\lambda_1 - \lambda_2}{1 + 10^{(pH-pK)}}$$

where λ_1 and λ_2 are the beginning and the end of the transition, respectively, and *pK* – is the midpoint of the transition.

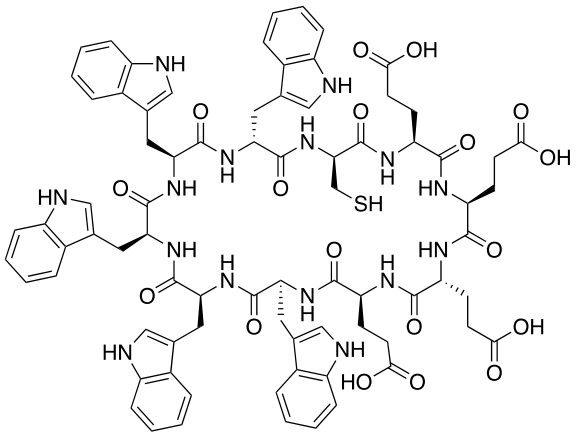

c[E_4W_5C]
Chemical Formula: $C_{78}H_{83}N_{15}O_{18}S$
Molecular Weight: 1550.67

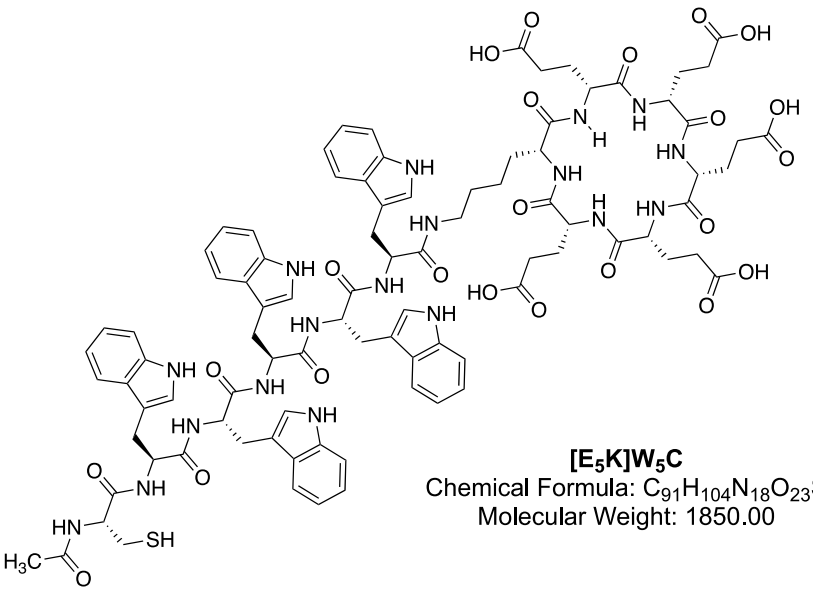

[E_5K]W_5C
Chemical Formula: $C_{91}H_{104}N_{18}O_{23}S$
Molecular Weight: 1850.00

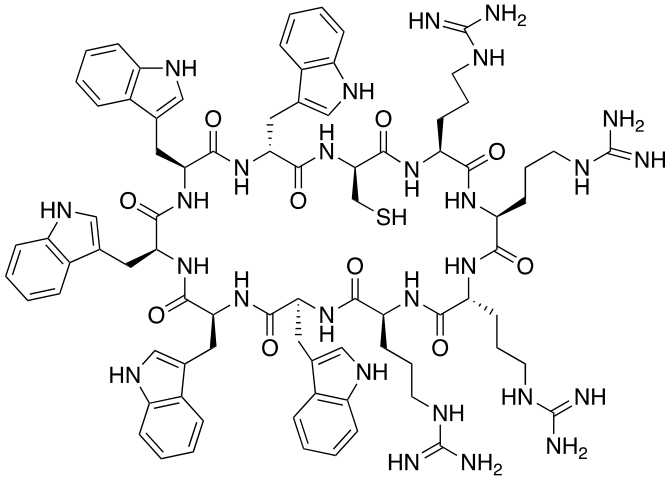

c[R_4W_5C]
Chemical Formula: $C_{82}H_{103}N_{27}O_{10}S$
Molecular Weight: 1658.97

Sequence: GCDNNEGFFATLGGEIPLWSDVVLAIEG
pHLIP-HM2A
Chemical Formula: $C_{131}H_{195}N_{31}O_{43}$
Molecular Weight: 2924.19

Supplemental Fig. 1. Sequence and structure of pHLIP and pHLIC peptides.

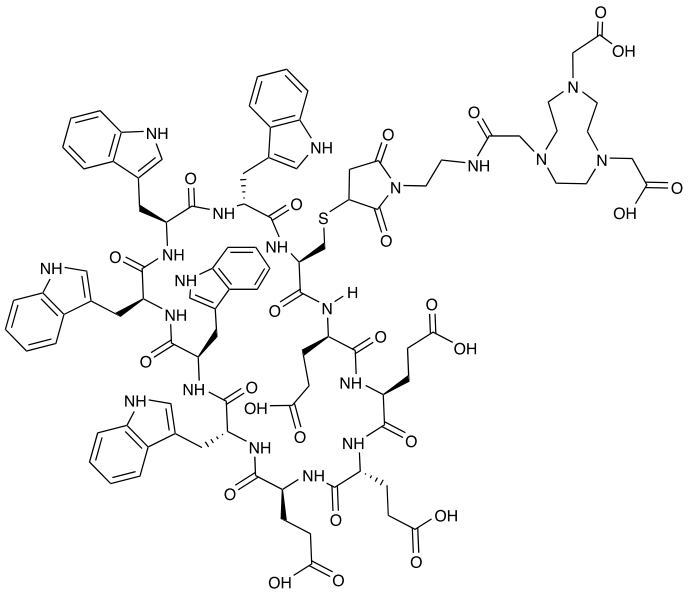

c[E_4W_5C]-NO2A
Chemical Formula: $C_{96}H_{110}N_{20}O_{25}S$
Molecular Weight: 1976.11

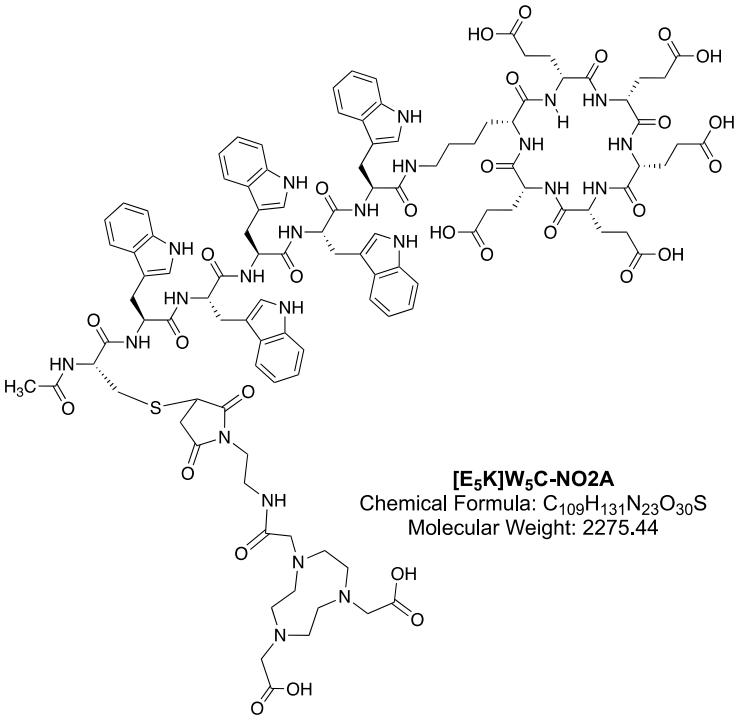

[E_5K]W_5C-NO2A
Chemical Formula: $C_{109}H_{131}N_{23}O_{30}S$
Molecular Weight: 2275.44

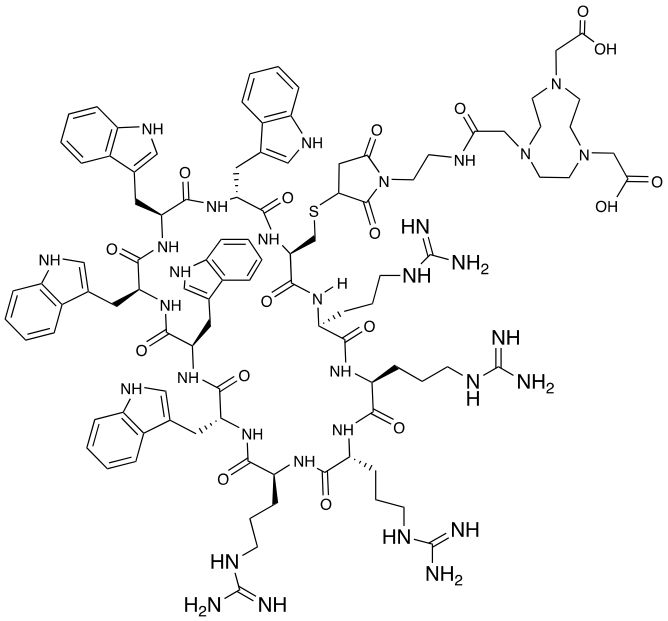

c[R_4W_5C]-NO2A
Chemical Formula: $C_{100}H_{130}N_{32}O_{17}S$
Molecular Weight: 2084.41

Supplemental Fig. 2. Structure of pHLIC-NO2A peptide conjugates.

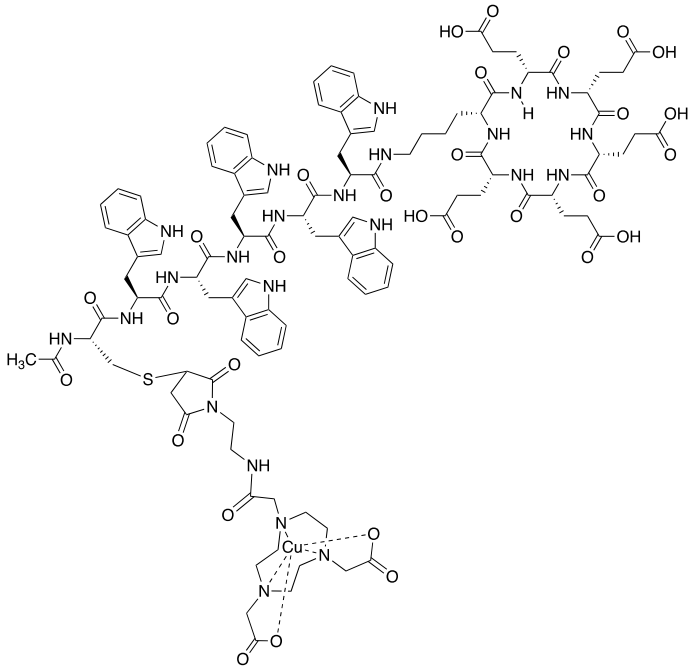

[^{64}Cu]Cu-NO2A-[E_5K]W_5C

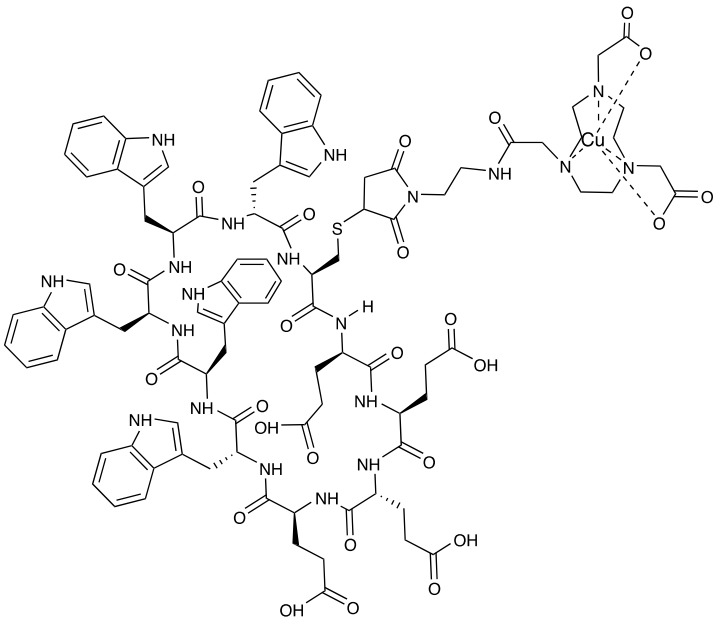

[^{64}Cu]Cu-NO2A-c[E_4W_5C]

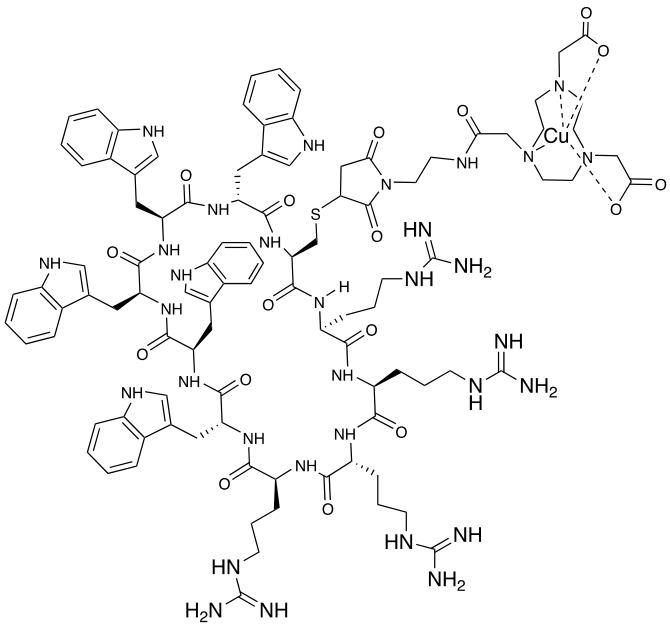

[^{64}Cu]Cu-NO2A-c[R_4W_5C]

Supplemental Fig. 3. Structure of ^{64}Cu-labelled pHLIC-NO2A peptide conjugates.

‡**Supplemental Fig. 4**. Instant thin-layer chromatography quality control of all ^{64}Cu-labelled pHLIC/pHLIP radiotracers.

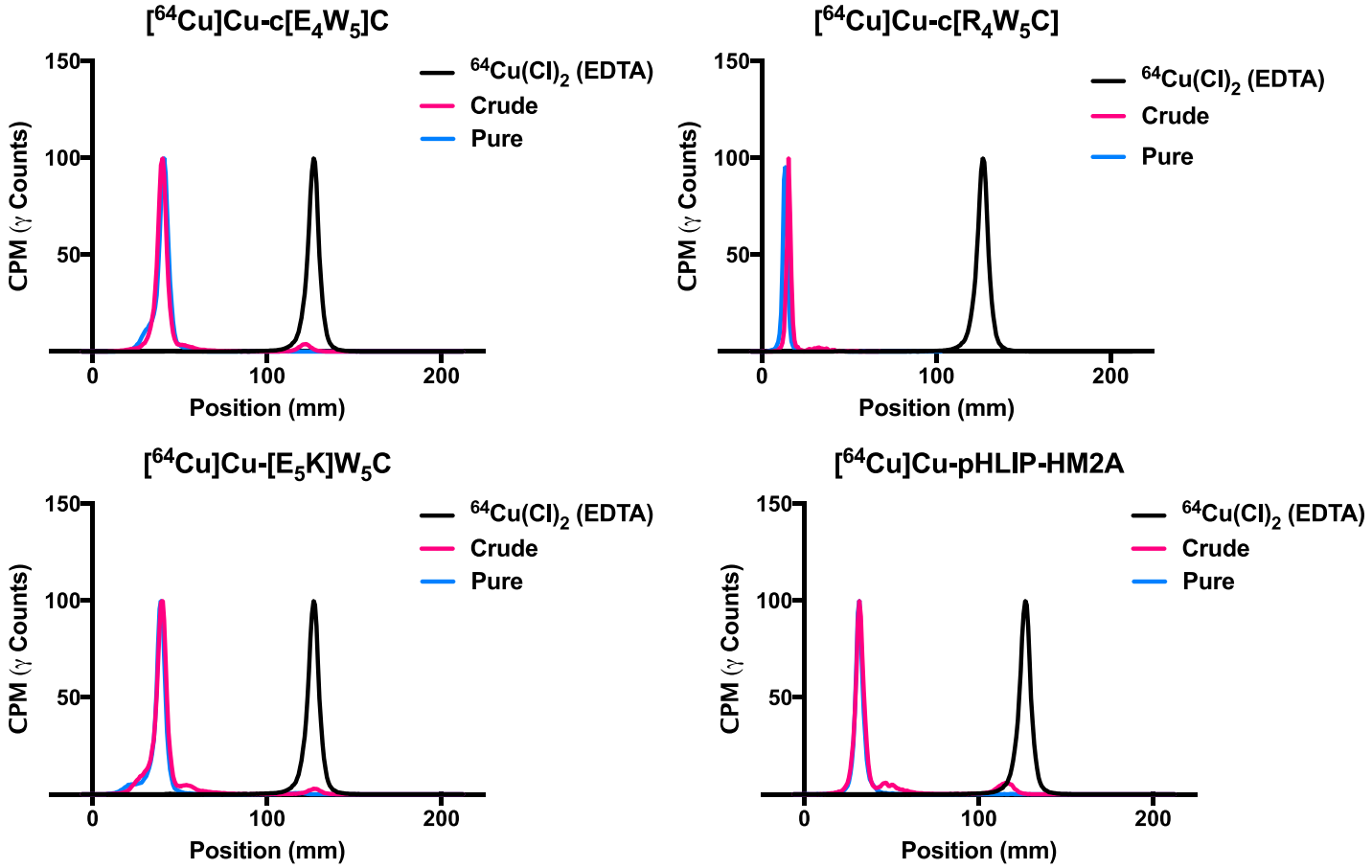

‡**Supplemental Table 1**. Experimentally determined LogP values of ^{64}Cu-labelled pHLIC/pHLIP radiotracers.

Compound	LogD (pH 6)			LogD (pH 7.4)		
[^{64}Cu]Cu-HM2A	-1.9	±	0.1	-2.2	±	0.3
[^{64}Cu]Cu-c[E_4W_5C]	2.5	±	0.1	2	±	0.2
[^{64}Cu]Cu-[E_5K]W_5C	2.1	±	0.1	2.3	±	0.3

‡**Supplemental Fig. 5**. Serum stability of ^{64}Cu-labelled pHLIC radiotracers (*n* = 3).

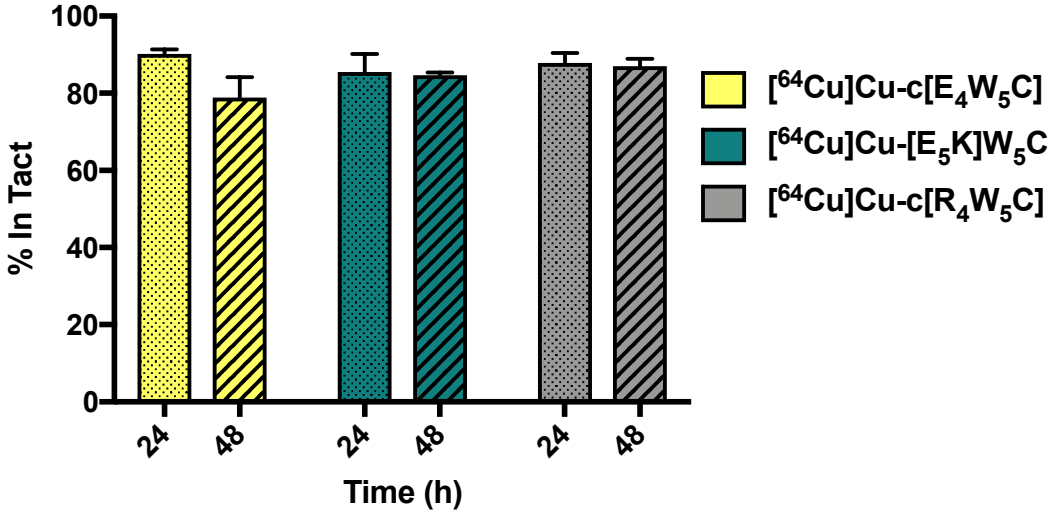

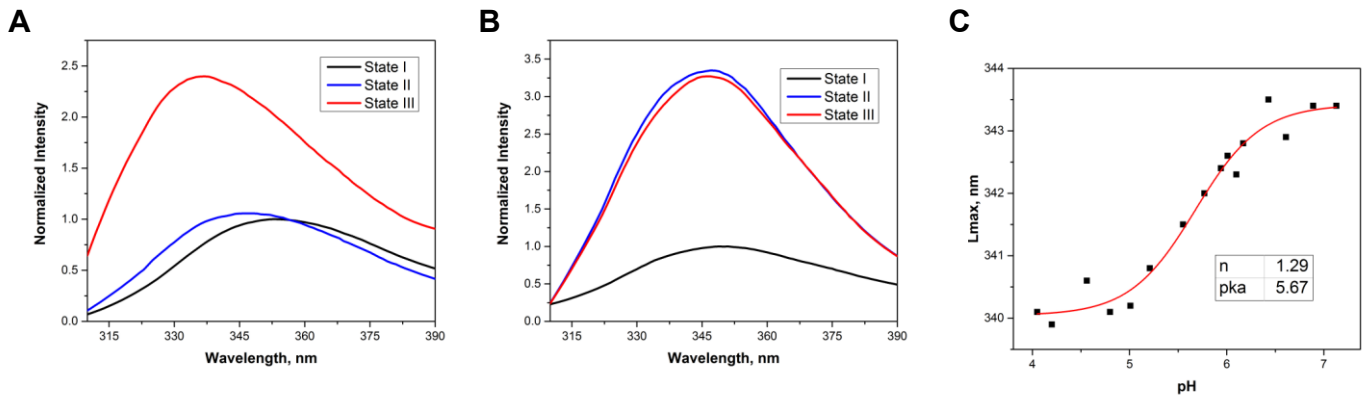

Supplemental Fig. 6. Tryptophan fluorescence spectra are shown from [^{nat}Cu]Cu-c[E$_4$W$_5$C] (A) and [^{nat}Cu]Cu-c[R$_4$W$_5$C] (B) in aqueous solution at pH 8 (black lines), at pH 8 in the presence of POPC liposomes (blue lines) and at pH 4 in the presence of POPC liposomes (red lines). The pH-dependent partition of [^{nat}Cu]Cu-c[E$_4$W$_5$C] into the lipid bilayers of POPC liposomes was studied by monitoring the changes in the position of maxima of fluorescence spectra as function of pH (C). The data were fitted using the Henderson-Hasselbalch equation, the fitting curves and 95% confidence interval are shown by red and pink areas, respectively.

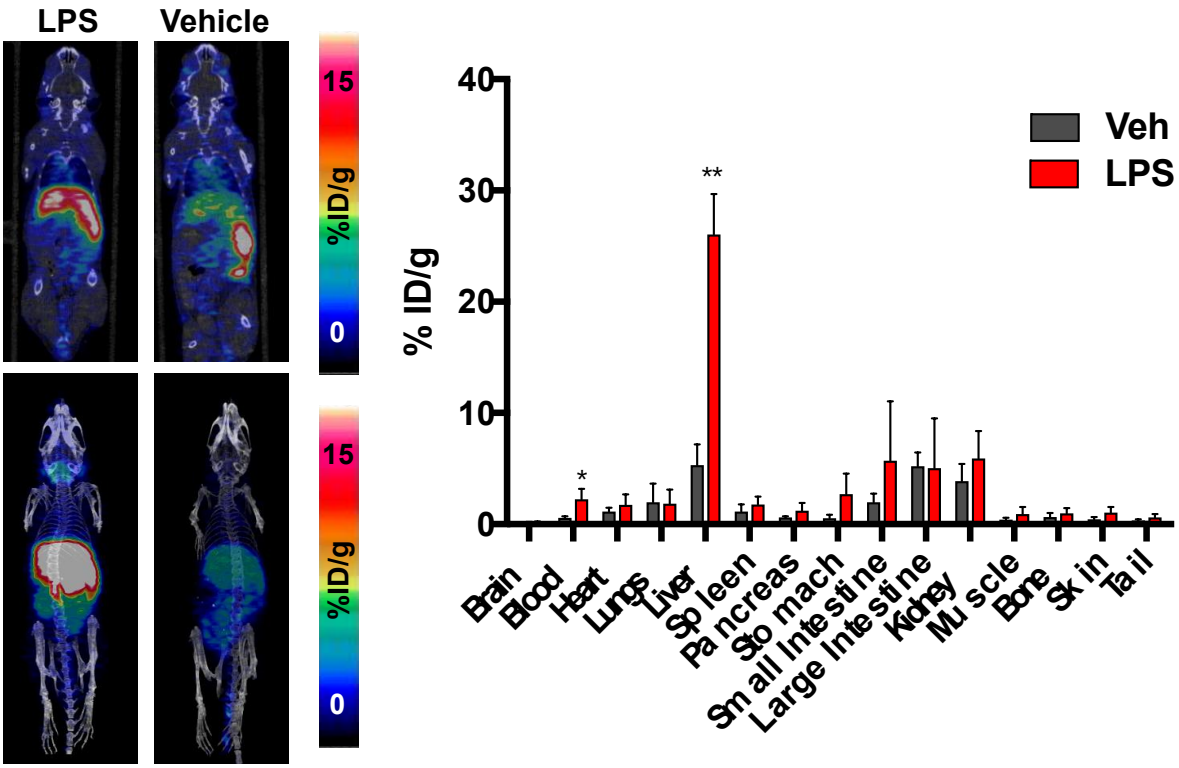

†**Supplemental Fig. 7**. PET imaging of [^{64}Cu]Cu-[E$_5$K]W$_5$C peptide and corresponding biodistribution at 24 h. The top panel represents coronal slices of the mice and the bottom panel represents the maximum intensity projections (MIPs). Data is represented as average %ID/g ± SD with *n* = 3-4 animals/group.

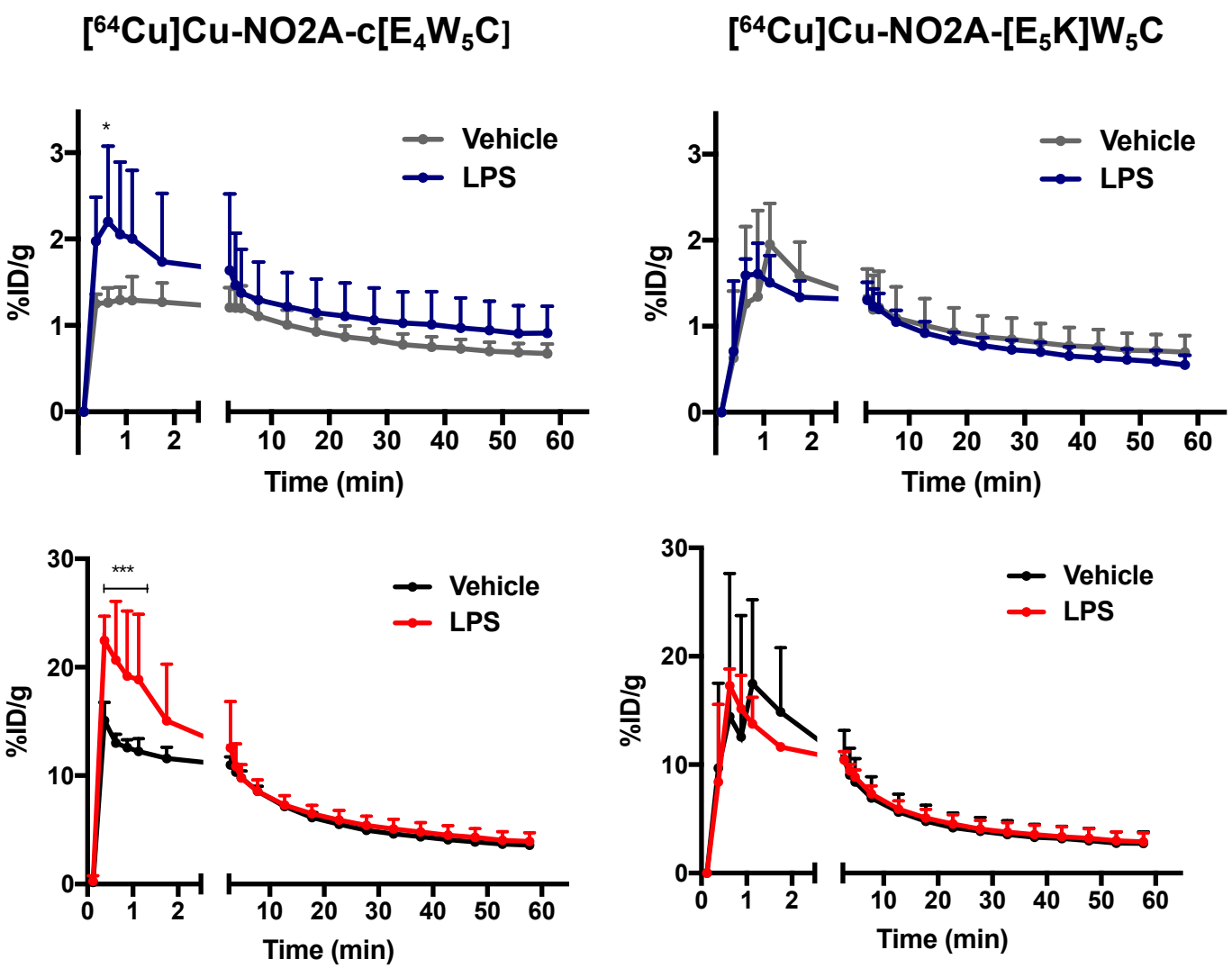

†**Supplemental Fig. 8**. Dynamic PET quantitation for the blood (top figures, red and black) and brain (bottom figures, blue and gray) uptake [^{64}Cu]Cu-NO2A-c[E_4W_5C] and [^{64}Cu]Cu-NO2A-[E_5K]W_5C pHLIC peptides. Data is represented as average %ID/g ± SD with *n* = 4 animals/group.

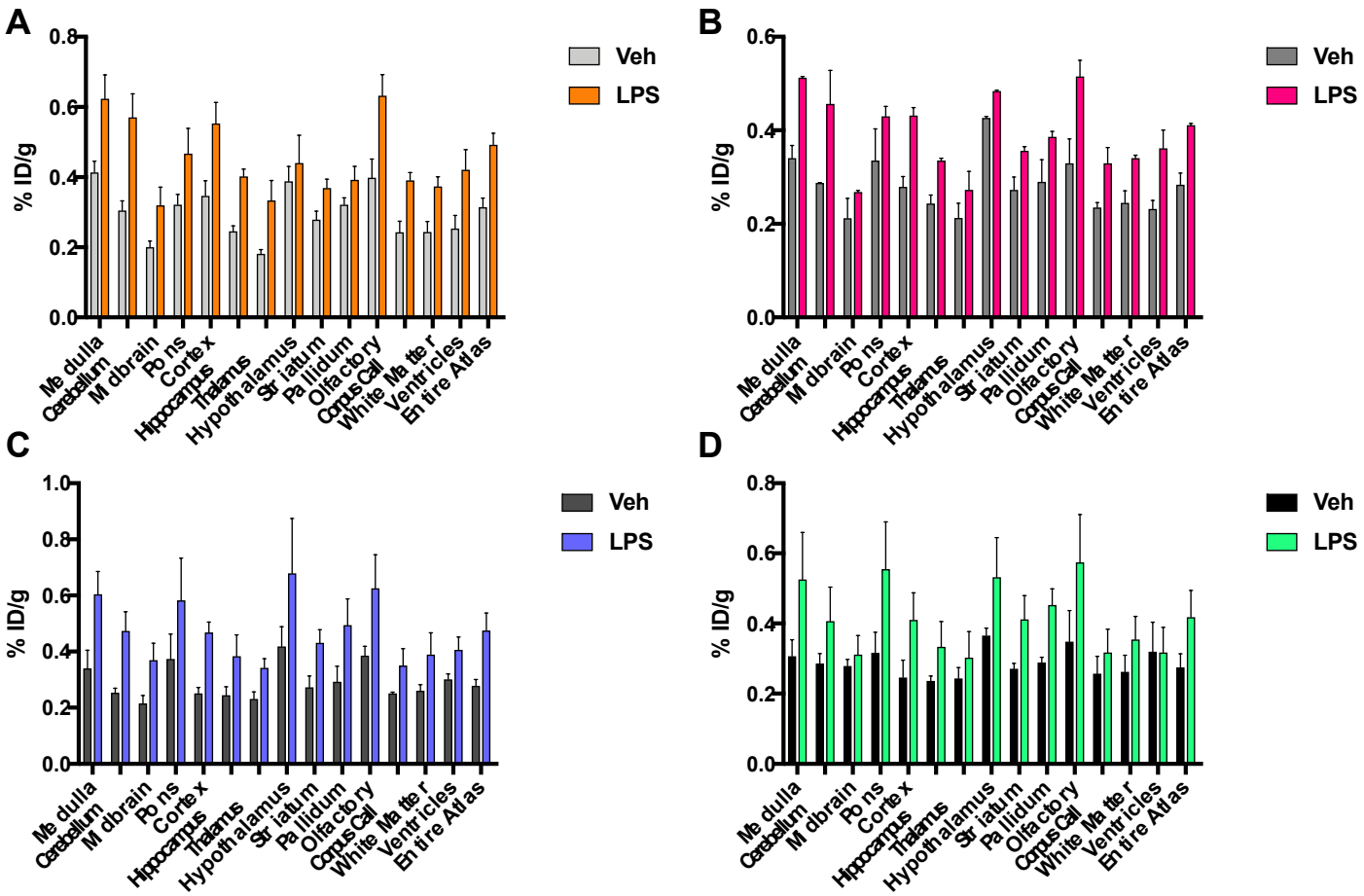

†**Supplemental Fig. 9**. Full brain PET quantitation of [^{64}Cu]Cu-NO2A-c[E_4W_5C] at 4 h (A), 8 h (B), 12 h (C), and 24 h (D) post-LPS injection corresponding with values tabulated in Supporting Table 4. Data is represented as average %ID/g ± SD with *n* = 4 animals/group.

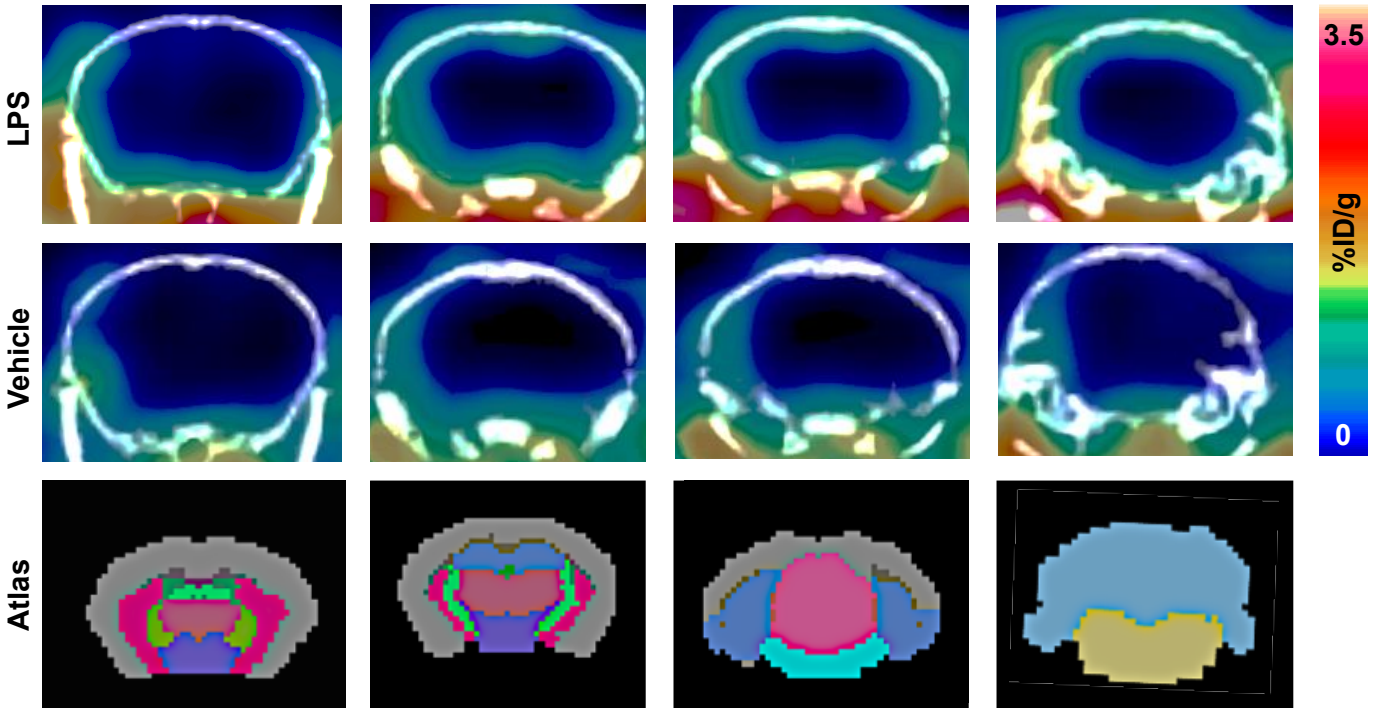

†**Supplemental Fig. 10**. Representative brain PET images of [^{64}Cu]Cu-NO2A-c[E_4W_5C] 4 h post-LPS injection (*n* = 4/group).

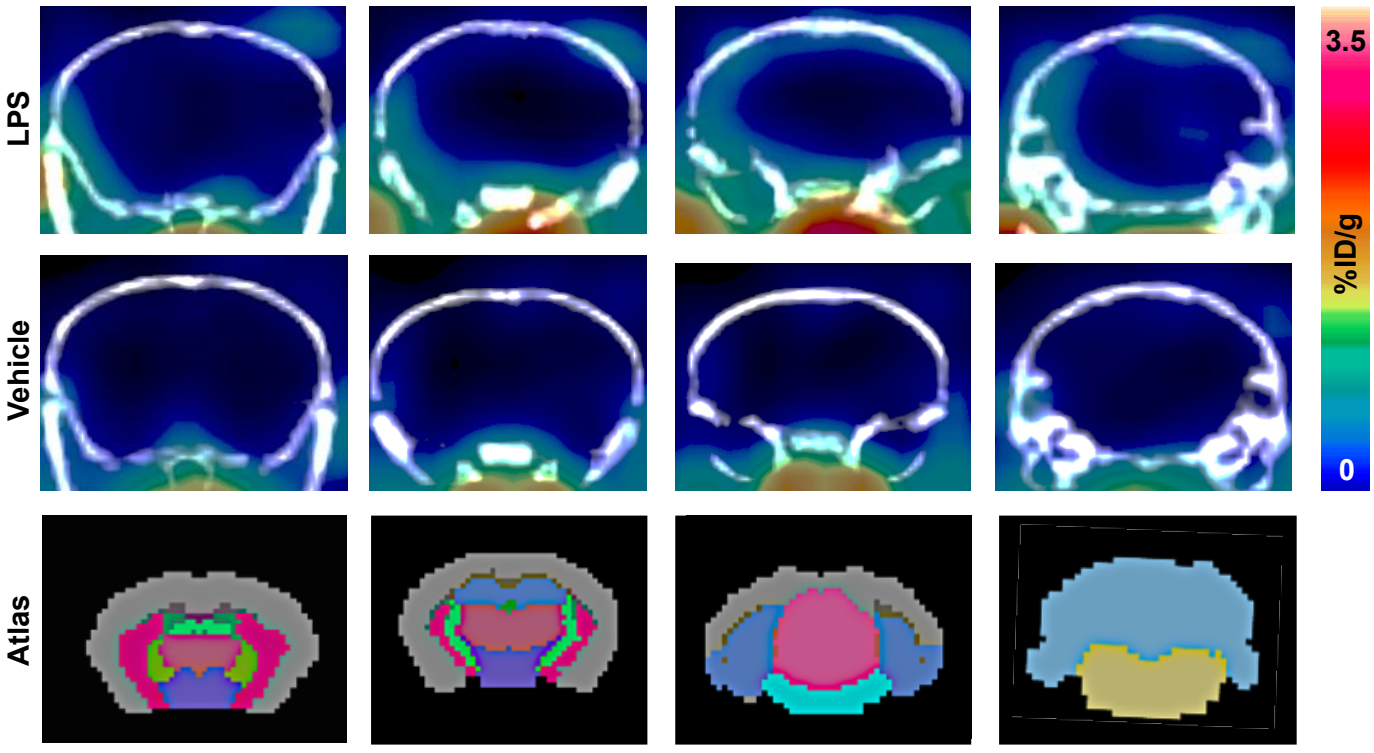

†**Supplemental Fig. 11**. Representative brain PET images of [^{64}Cu]Cu-NO2A-c[E_4W_5C] 8 h post-LPS injection (*n* = 4/group).

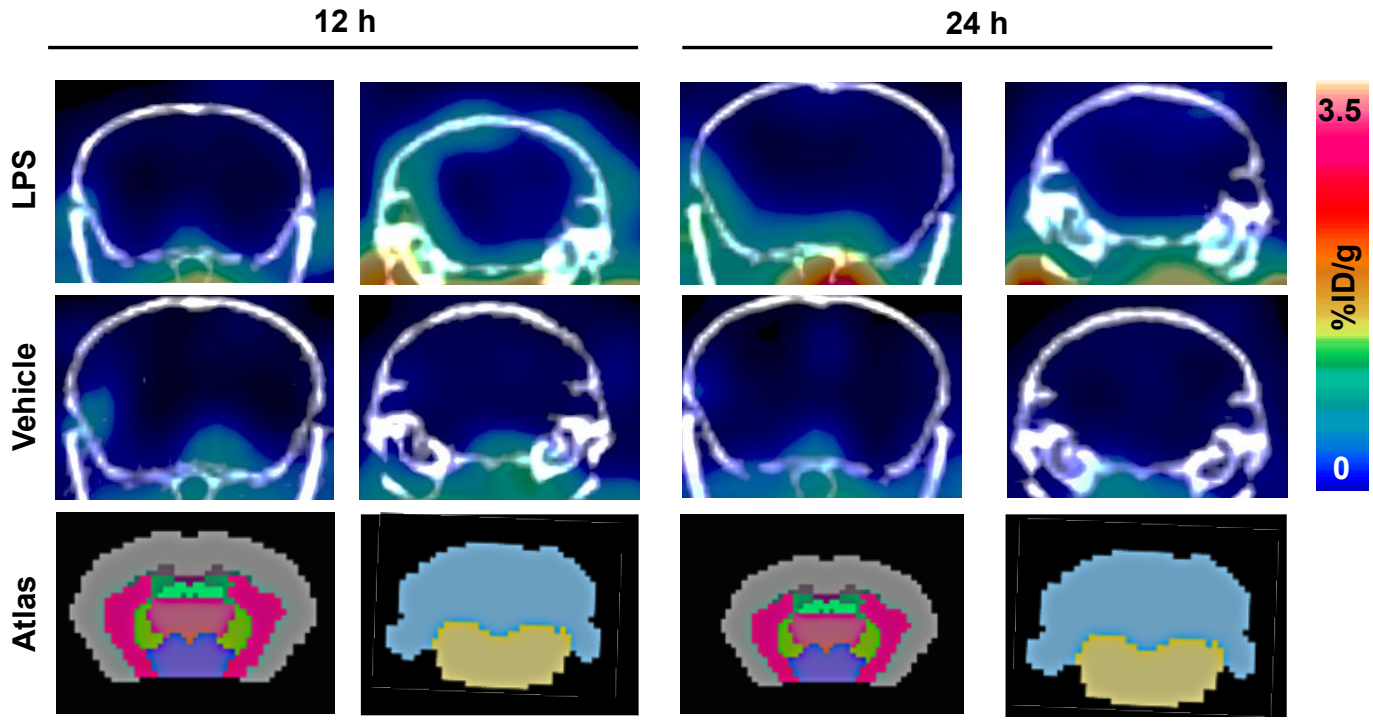

†**Supplemental Fig. 12**. Representative brain PET images of [^{64}Cu]Cu-NO2A-c[E_4W_5C] at 12 and 24 h-post injection with LPS. These views are showing the same representative mice shown in Fig. 4, but with additional views of the frontal cortex and cerebellum (*n* = 4/group).

Supplemental Fig. 13. Legend for inviCRO brain atlas represents segmentation algorithm used for PET quantitation.

Medulla
Cerebellum
Midbrain
Pons
Cortex
Hippocampus
Thalamus
Hypothalamus
Striatum
Pallidum
Olfactory
Corpus Callosum
White Matter
Ventricles

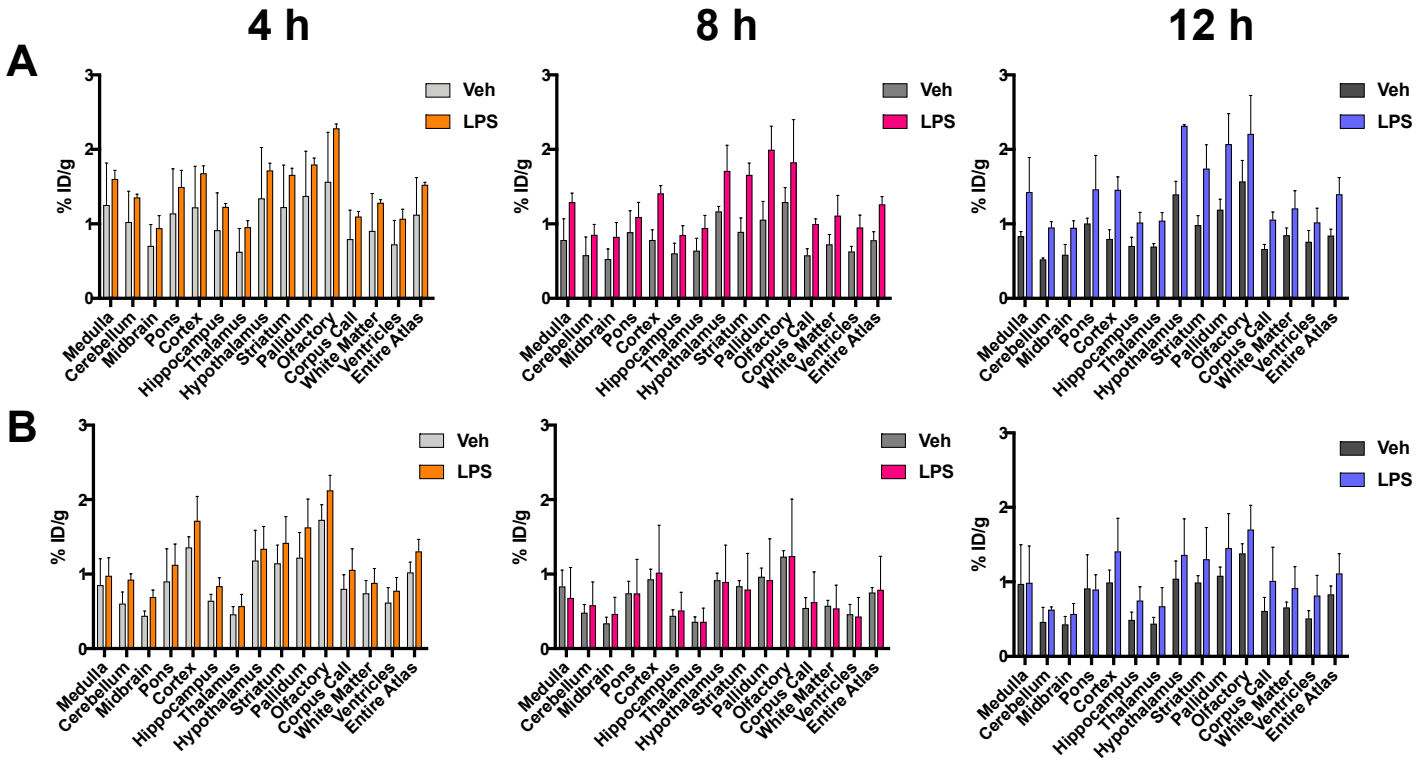

‡**Supplemental Fig. 14**. Full brain PET quantitation of and [^{64}Cu]Cu-NO2A-c[E$_4$W$_5$C] (A) and [^{64}Cu]Cu-NO2A-c[R$_4$W$_5$C] (B) at 4 h, 8 h, and 12 h post-LPS injection corresponding with values tabulated in Supporting Table 7. Data is represented as average %ID/g ± SD with *n* = 4 animals/group.

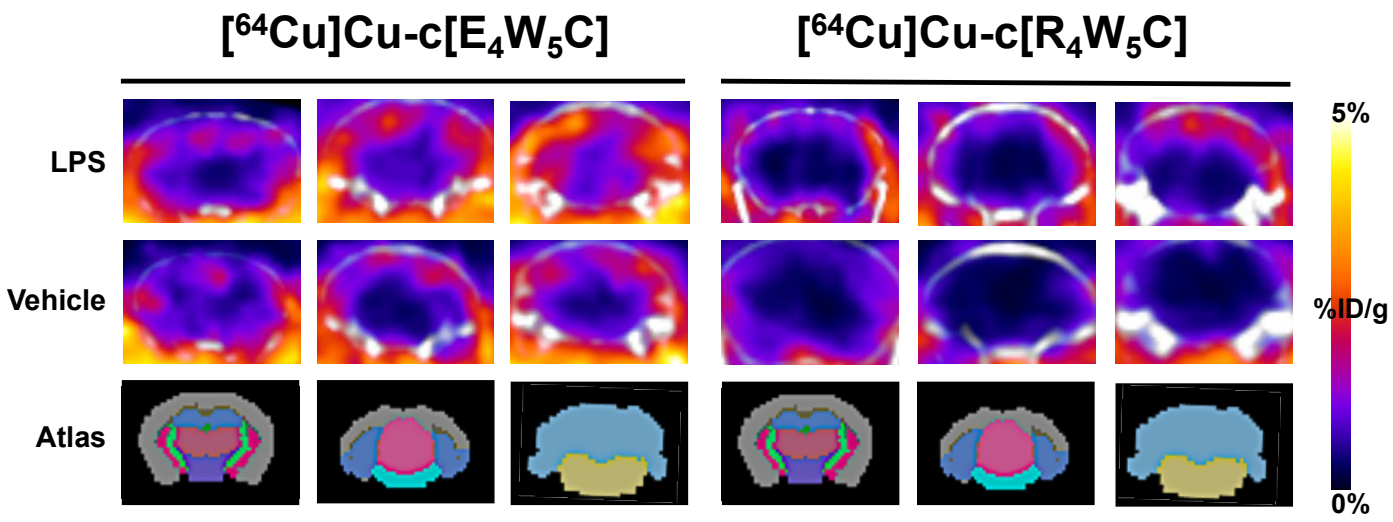

‡**Supplemental Fig. 15**. Representative brain PET images of [^{64}Cu]Cu-NO2A-c[E_4W_5C] vs. [^{64}Cu]Cu-NO2A-c[R_4W_5C] 4 h post-injection with LPS (selected from groups of *n* = 4).

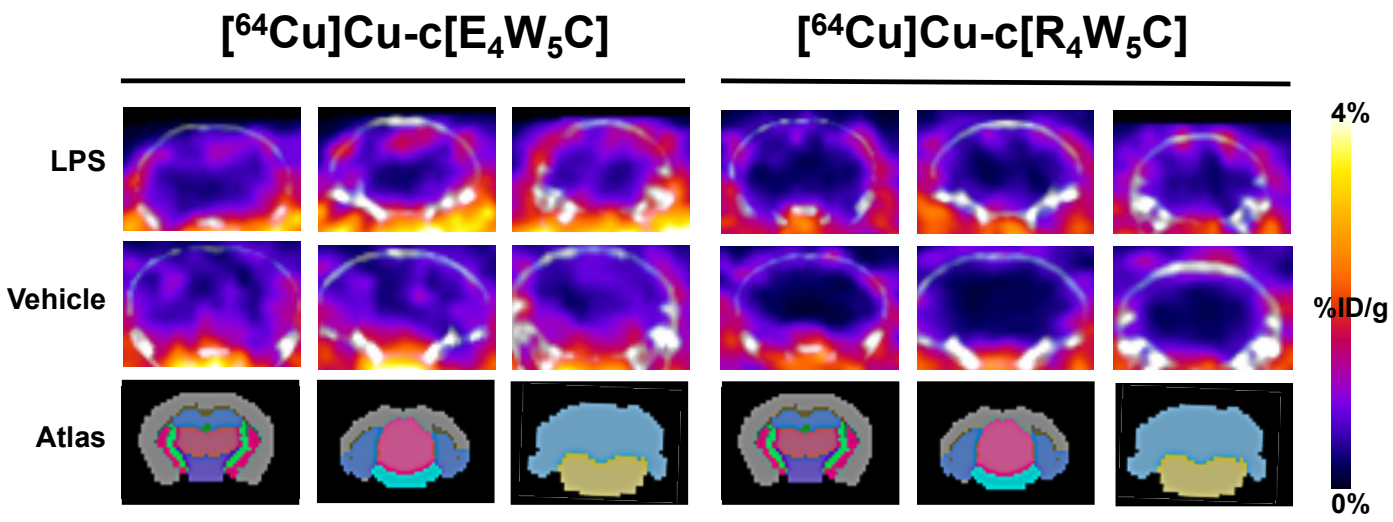

‡**Supplemental Fig. 16**. Representative brain PET images of [^{64}Cu]Cu-NO2A-c[E_4W_5C] vs. [^{64}Cu]Cu-NO2A-c[R_4W_5C] 8 h post-injection with LPS (selected from groups of *n* = 4).

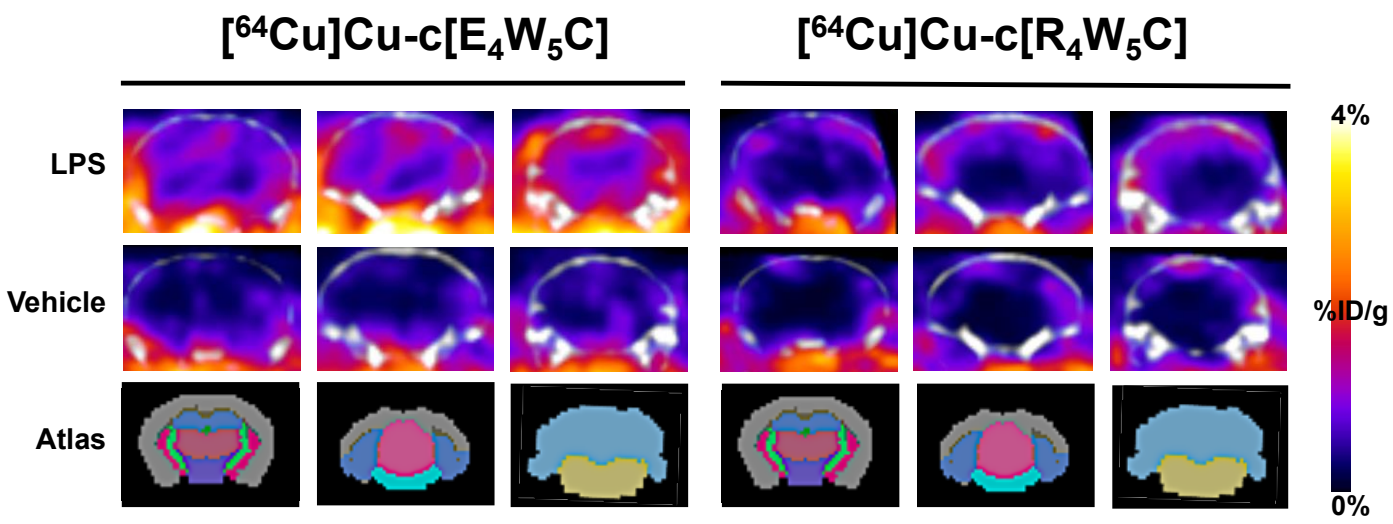

‡**Supplemental Fig. 17**. Representative brain PET images of [^{64}Cu]Cu-NO2A-c[E_4W_5C] vs. [^{64}Cu]Cu-NO2A-c[R_4W_5C] 12 h post-injection with LPS (selected from groups of *n* = 4).

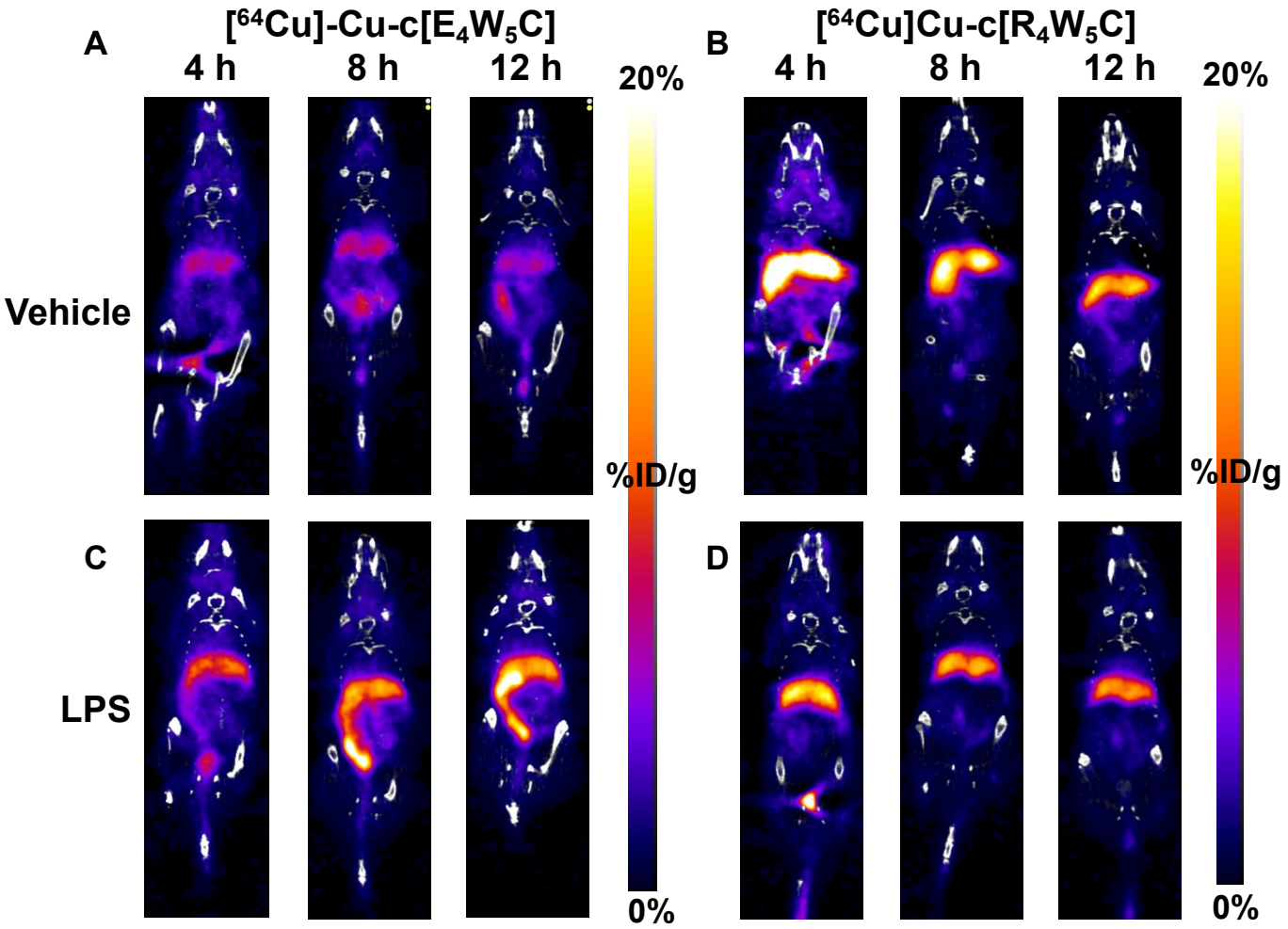
A
[64Cu]-Cu-c[E4W5C]
4 h
8 h
12 h
20%
B
[64Cu]Cu-c[R4W5C]
4 h
8 h
12 h
20%
Vehicle
%ID/g
%ID/g
C
D
LPS
0%
0%

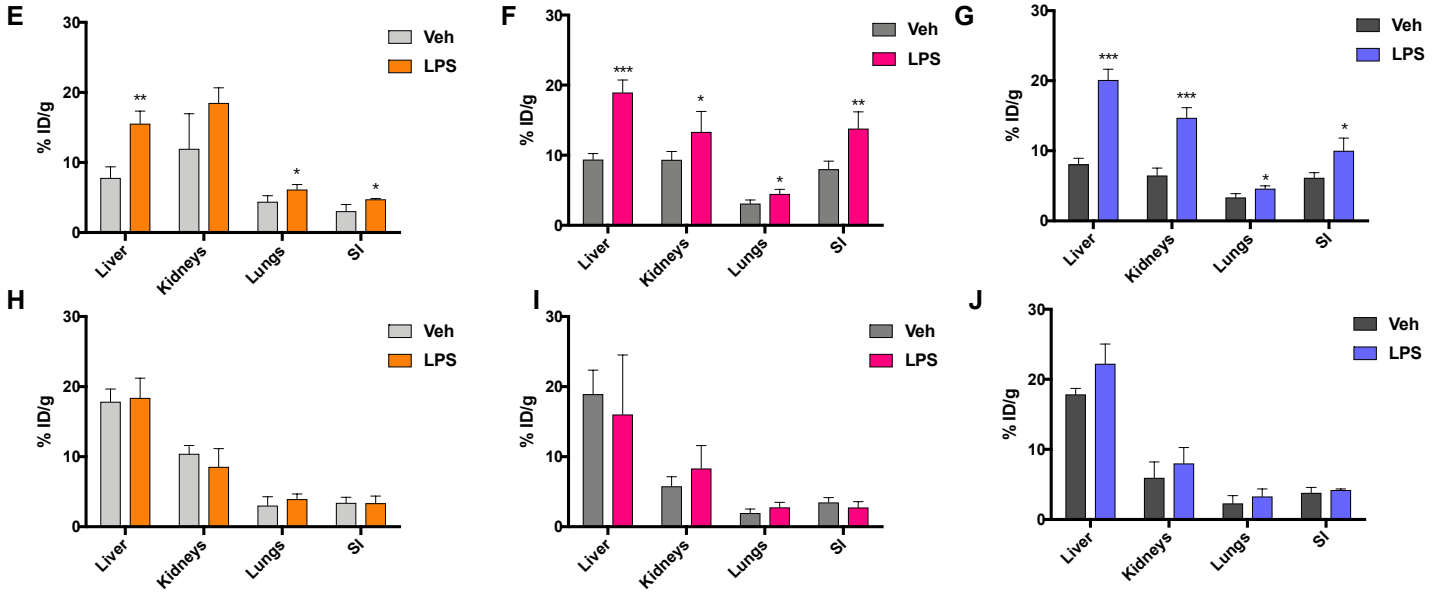
E
F
G
H
I
J
% ID/g
Veh
LPS
Liver
Kidneys
Lungs
SI

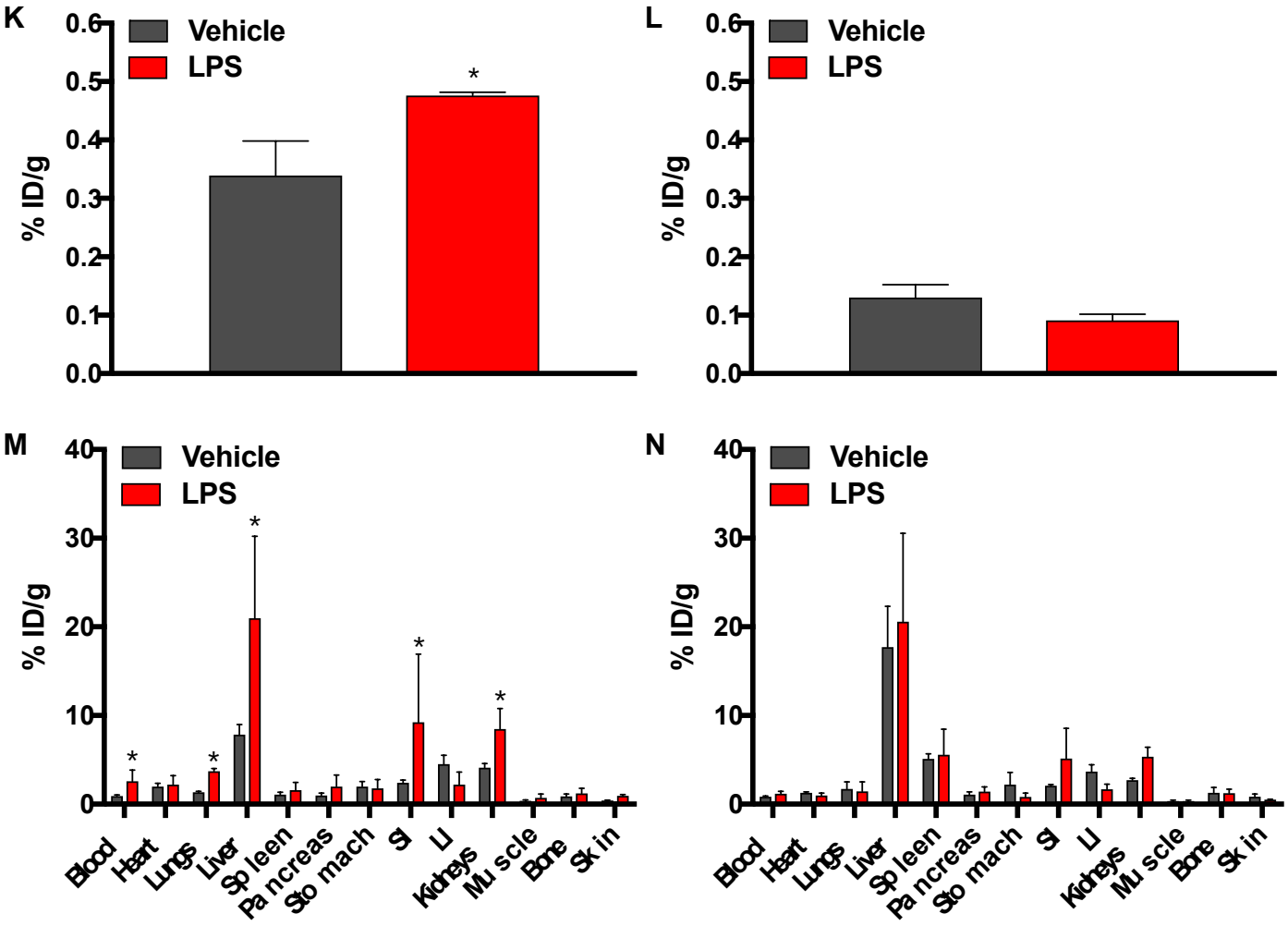

‡**Supplemental Fig. 18**. Serial PET imaging of [^{64}Cu]Cu-c[E_4W_5C] vs. [^{64}Cu]Cu-c[R_4W_5C] uptake in vehicle (A and B) vs. LPS-treated (C and D) mice over the course of 12 h (*n* = 4/group). Peripheral quantitation of PET organs was performed by manually drawing ROIs around select tissues at 4 h, 8 h, and 12 h post-LPS inoculation for [^{64}Cu]Cu-c[E_4W_5C] (E, F, and G, respectively) and [^{64}Cu]Cu-c[R_4W_5C] at 4 h, 8 h, and 12 h post-LPS (H, I, and J, respectively). Full biodistribution was performed at 24 h post-LPS injection (*n* = 4/group for vehicle, *n* = 2/LPS for group, per radiotracer). Brain uptake (K) and respective whole-body values (M) are shown for [^{64}Cu]Cu-c[E_4W_5C] pHLIC. Brain uptake (L) and respective values (N) are shown for [^{64}Cu]Cu-c[R_4W_5C] control. Tabulated values for peripheral PET and ex vivo biodistribution can be found in Supplemental Tables 8 and 9.

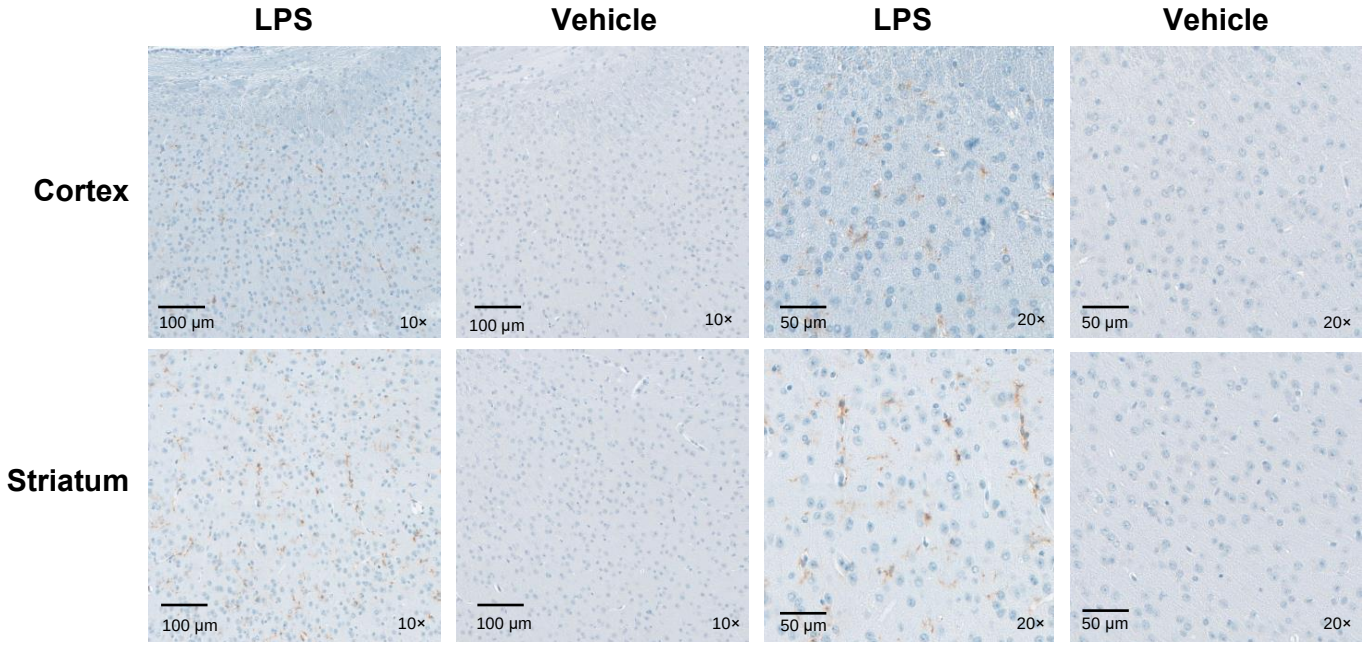

‡**Supplemental Fig. 19**. Immunohistochemical staining of TMEM119 show an increase in microglia in select brain regions of LPS-treated mice vs. vehicle (*n* = 3/group).

†**Supplemental Table 2**. Full ex vivo biodistribution of [^{64}Cu]Cu-[E_5K]W_5C at 24 h. Data is represented as average %ID/g ± SD with *n* = 4 animals/group. Abbreviations: SI: small intestine; LI: large intestine.

24 h			
Tissue	Vehicle	LPS	P value
Brain	0.14 ± 0.03	0.20 ± 0.06	0.134697
Blood	0.60 ± 0.11	2.23 ± 0.96	0.017429
Heart	1.13 ± 0.33	1.76 ± 0.93	0.256697
Lungs	2.00 ± 1.66	1.83 ± 1.29	0.893041
Liver	5.30 ± 1.87	26.06 ± 3.63	0.00017
Spleen	1.14 ± 0.63	1.77 ± 0.71	0.26613
Pancreas	0.61 ± 0.10	1.22 ± 0.69	0.114409
Stomach	0.54 ± 0.32	2.70 ± 1.86	0.065958
SI	1.98 ± 0.76	5.72 ± 5.32	0.19078
LI	5.20 ± 1.24	5.04 ± 4.48	0.946782
Kidneys	3.87 ± 1.55	5.92 ± 2.48	0.234547
Muscle	0.43 ± 0.14	0.93 ± 0.61	0.160568
Bone	0.66 ± 0.36	0.99 ± 0.46	0.332227
Skin	0.44 ± 0.21	1.03 ± 0.50	0.081138
Tail	0.36 ± 0.09	0.63 ± 0.29	0.13116

‡**Supplemental Table 3**. Full ex vivo biodistribution of [^{64}Cu]Cu-c[E_4W_5C] at 12 and 24 h (*n* = 4/group) with respective P values (as determined by unpaired two-tailed t-test) comparing vehicle and LPS-treated groups. Data is represented as average %ID/g ± SD with *n* = 4 animals/group.

12 h			
Tissue	Vehicle	LPS	P value
Brain	0.20 ± 0.05	0.25 ± 0.06	0.353235
Blood	1.08 ± 0.09	2.73 ± 1.43	0.117516
Heart	1.79 ± 0.42	2.71 ± 0.45	0.061524
Lungs	1.95 ± 0.62	2.82 ± 0.64	0.305098
Liver	10.24 ± 1.41	12.68 ± 3.71	0.34753
Spleen	2.60 ± 0.84	3.37 ± 0.30	0.205689
Pancreas	1.32 ± 0.41	2.29 ± 0.32	0.032566
Stomach	3.52 ± 1.66	3.20 ± 1.08	0.791259
SI	5.07 ± 1.04	11.71 ± 4.73	0.07658
LI	14.14 ± 2.94	4.60 ± 0.73	0.005475
Kidneys	7.13 ± 1.30	13.27 ± 2.54	0.020305
Muscle	0.31 ± 0.23	1.07 ± 0.15	0.008741
Bone	0.72 ± 0.16	1.34 ± 0.36	0.052285
Skin	1.35 ± 0.14	2.78 ± 1.46	0.164904

24 h			
Tissue	Vehicle	LPS	P value
Brain	0.29 ± 0.05	0.43 ± 0.04	0.000308
Blood	1.29 ± 0.27	3.60 ± 1.77	0.009368
Heart	2.35 ± 0.45	2.54 ± 0.45	0.469931
Lungs	1.94 ± 0.84	3.79 ± 1.49	0.032256
Liver	12.07 ± 1.56	23.84 ± 5.32	0.000793
Spleen	2.64 ± 0.92	3.80 ± 1.23	0.085074
Pancreas	1.24 ± 0.36	2.47 ± 0.85	0.007407
Stomach	1.59 ± 0.94	2.66 ± 1.81	0.222081
SI	4.36 ± 1.33	15.75 ± 6.78	0.002016
LI	10.04 ± 3.57	5.41 ± 4.18	0.057131
Kidneys	7.17 ± 1.98	9.74 ± 0.81	0.009285
Muscle	0.70 ± 0.26	1.19 ± 0.29	0.01123
Bone	1.23 ± 0.36	1.43 ± 0.53	0.468761
Skin	1.17 ± 0.27	2.47 ± 0.71	0.00139

†**Supplemental Table 4**. PET quantitation of [^{64}Cu]Cu-c[E_4W_5C] of select regions at 4, 8, 12, and 24 h post-LPS injection. Data is represented as average %ID/g ± SD with *n* = 4 animals/group. Abbreviations: SI: small intestine; LI: large intestine.

24 h			
Tissue	Vehicle	LPS	P value
Liver	5.99 ± 0.47	13.12 ± 2.91	7.34E-05
SI	5.26 ± 0.57	13.20 ± 3.68	0.000229
Kidneys	3.17 ± 0.62	6.59 ± 1.70	0.000562
Lungs	1.25 ± 0.13	1.99 ± 0.36	0.000419

12 h			
Tissue	Vehicle	LPS	P value
Liver	6.56 ± 0.99	13.63 ± 1.81	0.000473
SI	5.86 ± 0.65	12.07 ± 1.68	0.00046
Kidneys	5.90 ± 2.61	10.80 ± 2.49	0.035003
Lungs	1.18 ± 0.02	2.24 ± 0.38	0.001443

8 h			
Tissue	Vehicle	LPS	P value
Liver	9.00 ± 0.26	15.64 ± 0.58	8.14E-07
SI	8.66 ± 0.13	16.70 ± 1.15	8.81E-06
Kidneys	6.34 ± 0.74	11.03 ± 0.29	2.22E-05
Lungs	1.22 ± 0.06	2.06 ± 0.11	1.43E-05

4 h			
Tissue	Vehicle	LPS	P value
Liver	8.99 ± 2.37	18.49 ± 4.77	0.011877
SI	8.08 ± 2.23	16.83 ± 5.04	0.019203
Kidneys	8.46 ± 2.22	14.08 ± 3.62	0.058369
Lungs	1.73 ± 0.44	3.35 ± 0.88	0.01618

†**Supplemental Table 5**. Full PET quantitation of brain regions at 4, 8, 12, and 24 h post-LPS injection for [^{64}Cu]Cu-c[E_4W_5C]. Data is represented as average %ID/g ± SD with *n* = 4 animals/group. Abbreviations: Corpus Call: Corpus Callosum.

24 h			
Tissue	Vehicle	LPS	P value
Medulla	0.41 ± 0.12	0.76 ± 0.06	0.0018
Cerebellum	0.36 ± 0.07	0.56 ± 0.09	0.0265
Midbrain	0.30 ± 0.03	0.48 ± 0.09	0.0113
Pons	0.37 ± 0.08	0.75 ± 0.10	<0.0001
Cortex	0.28 ± 0.04	0.53 ± 0.08	0.0025
Hippocampus	0.29 ± 0.05	0.48 ± 0.10	0.0452
Thalamus	0.31 ± 0.07	0.42 ± 0.08	0.97
Hypothalamus	0.42 ± 0.07	0.90 ± 0.18	<0.0001
Striatum	0.34 ± 0.07	0.53 ± 0.07	0.0914
Pallidum	0.35 ± 0.06	0.62 ± 0.10	0.001
Olfactory	0.37 ± 0.05	0.62 ± 0.11	0.0098
Corpus Call	0.32 ± 0.06	0.45 ± 0.07	0.5863
White Matter	0.31 ± 0.05	0.49 ± 0.07	0.1875
Ventricles	0.39 ± 0.09	0.48 ± 0.06	0.9834
Entire Atlas	0.33 ± 0.05	0.56 ± 0.08	0.0067

12 h			
Tissue	Vehicle	LPS	P value
Medulla	0.34 ± 0.0643	0.60 ± 0.0805	<0.0001
Cerebellum	0.25 ± 0.0155	0.47 ± 0.0681	0.0005
Midbrain	0.22 ± 0.0290	0.37 ± 0.0601	0.0418
Pons	0.37 ± 0.0880	0.58 ± 0.1498	0.0011
Cortex	0.25 ± 0.0206	0.47 ± 0.0373	0.0006
Hippocampus	0.24 ± 0.0297	0.38 ± 0.0758	0.097
Thalamus	0.23 ± 0.0252	0.34 ± 0.0323	0.3633
Hypothalamus	0.42 ± 0.0706	0.68 ± 0.1957	<0.0001
Striatum	0.27 ± 0.0400	0.43 ± 0.0463	0.0318
Pallidum	0.29 ± 0.0551	0.49 ± 0.0934	0.0019
Olfactory	0.39 ± 0.0337	0.63 ± 0.1201	0.0001
Corpus Call	0.25 ± 0.0046	0.35 ± 0.0605	0.5486
White Matter	0.26 ± 0.0219	0.39 ± 0.0775	0.1633
Ventricles	0.30 ± 0.0194	0.41 ± 0.0456	0.4474
Entire Atlas	0.28 ± 0.0232	0.48 ± 0.0615	0.0024

8 h			
Tissue	Vehicle	LPS	P value
Medulla	0.34 ± 0.0269	0.51 ± 0.0023	<0.0001
Cerebellum	0.29 ± 0.0002	0.46 ± 0.0716	<0.0001
Midbrain	0.21 ± 0.0422	0.27 ± 0.0034	0.7013
Pons	0.34 ± 0.0678	0.43 ± 0.0213	0.0612
Cortex	0.28 ± 0.0221	0.43 ± 0.0168	0.0003
Hippocampus	0.24 ± 0.0184	0.34 ± 0.0047	0.0736
Thalamus	0.21 ± 0.0317	0.27 ± 0.0395	0.5882
Hypothalamus	0.43 ± 0.0032	0.48 ± 0.0016	0.6548
Striatum	0.27 ± 0.0278	0.36 ± 0.0089	0.1404
Pallidum	0.29 ± 0.0472	0.39 ± 0.0114	0.0535
Olfactory	0.33 ± 0.0518	0.52 ± 0.0342	<0.0001
Corpus Call	0.24 ± 0.0105	0.33 ± 0.0331	0.0587
White Matter	0.25 ± 0.0255	0.34 ± 0.0060	0.056
Ventricles	0.23 ± 0.0182	0.36 ± 0.0390	0.0029
Entire Atlas	0.28 ± 0.0250	0.41 ± 0.0038	0.0034

4 h			
Tissue	Vehicle	LPS	P value
Medulla	0.41 ± 0.0323	0.62 ± 0.0681	<0.0001
Cerebellum	0.30 ± 0.0278	0.57 ± 0.0677	<0.0001
Midbrain	0.20 ± 0.0175	0.32 ± 0.0522	0.003
Pons	0.32 ± 0.0299	0.47 ± 0.0719	0.0001
Cortex	0.35 ± 0.0432	0.55 ± 0.0599	<0.0001
Hippocampus	0.25 ± 0.0152	0.40 ± 0.0204	<0.0001
Thalamus	0.18 ± 0.0119	0.33 ± 0.0563	<0.0001
Hypothalamus	0.39 ± 0.0425	0.44 ± 0.0794	0.7646
Striatum	0.28 ± 0.0240	0.37 ± 0.0252	0.0611
Pallidum	0.32 ± 0.0192	0.39 ± 0.0388	0.3031
Olfactory	0.40 ± 0.0532	0.63 ± 0.0606	<0.0001
Corpus Call	0.24 ± 0.0315	0.39 ± 0.0224	<0.0001
White Matter	0.24 ± 0.0299	0.37 ± 0.0273	0.0009
Ventricles	0.25 ± 0.0370	0.42 ± 0.0576	<0.0001
Entire Atlas	0.31 ± 0.0259	0.49 ± 0.0327	<0.0001

‡**Supplemental Table 6**. A. Full PET quantitation of brain regions for [^{64}Cu]Cu-c[R_4W_5C] and [^{64}Cu]Cu-c[E_4W_5C] at 4, 8, and 12 h post-LPS injection. Data is represented as average %ID/g ± SD with *n* = 4 animals/group. Abbreviations: Corpus Call: Corpus Callosum. B. P values comparing LPS groups of [^{64}Cu]Cu-c[E_4W_5C] vs. LPS of [^{64}Cu]Cu-c[R_4W_5C].

A.

[^{64}Cu]Cu-c[E_4W_5]C 4 h			
Tissue	Vehicle	LPS	P value
Medulla	1.25 ± 0.5609	1.60 ± 0.1148	0.9867
Cerebellum	1.03 ± 0.4117	1.36 ± 0.0425	0.9925
Midbrain	0.71 ± 0.2843	0.94 ± 0.1681	0.9998
Pons	1.14 ± 0.5968	1.50 ± 0.2231	0.9851
Cortex	1.22 ± 0.5491	1.68 ± 0.0997	0.8847
Hippocampus	0.92 ± 0.5016	1.23 ± 0.0449	0.9953
Thalamus	0.63 ± 0.3106	0.96 ± 0.0875	0.9924
Hypothalamus	1.34 ± 0.6794	1.72 ± 0.0969	0.9755
Striatum	1.23 ± 0.5616	1.66 ± 0.0861	0.9208
Pallidum	1.38 ± 0.6004	1.80 ± 0.0854	0.9343
Olfactory	1.57 ± 0.6618	2.28 ± 0.0574	0.2632
Corpus Call	0.80 ± 0.3868	1.10 ± 0.0671	0.9968
White Matter	0.91 ± 0.4999	1.28 ± 0.0414	0.9731
Ventricles	0.73 ± 0.3198	1.07 ± 0.1294	0.9888
Entire Atlas	1.12 ± 0.4961	1.53 ± 0.0317	0.9544

[^{64}Cu]Cu-c[E_4W_5]C 8 h			
Tissue	**Vehicle**	**LPS**	**P value**
Medulla	0.78 ± 0.2847	1.29 ± 0.1236	0.068
Cerebellum	0.58 ± 0.2410	0.85 ± 0.1402	0.8532
Midbrain	0.53 ± 0.1328	0.83 ± 0.1918	0.875
Pons	0.89 ± 0.2858	1.09 ± 0.1944	0.9836
Cortex	0.78 ± 0.1364	1.41 ± 0.1048	0.0089
Hippocampus	0.61 ± 0.1341	0.85 ± 0.1243	0.9281
Thalamus	0.64 ± 0.1653	0.95 ± 0.1669	0.8495
Hypothalamus	1.17 ± 0.0641	1.71 ± 0.3452	0.0391
Striatum	0.89 ± 0.1870	1.66 ± 0.1595	0.0006
Pallidum	1.06 ± 0.2457	2.00 ± 0.3164	<0.0001
Olfactory	1.29 ± 0.1933	1.83 ± 0.5715	0.0447
Corpus Call	0.58 ± 0.0858	1.00 ± 0.0674	0.247
White Matter	0.73 ± 0.1295	1.11 ± 0.2685	0.3607
Ventricles	0.63 ± 0.0685	0.95 ± 0.1632	0.6392
Entire Atlas	0.78 ± 0.1146	1.26 ± 0.1011	0.0979

[^{64}Cu]Cu-c[E_4W_5]C 12 h			
Tissue	Vehicle	LPS	P value
Medulla	0.84 ± 0.0594	1.43 ± 0.4628	0.0263
Cerebellum	0.52 ± 0.0160	0.95 ± 0.0731	0.2657
Midbrain	0.59 ± 0.1377	0.95 ± 0.0930	0.5367
Pons	1.01 ± 0.0694	1.46 ± 0.4543	0.1885
Cortex	0.80 ± 0.1218	1.46 ± 0.1726	0.0083
Hippocampus	0.70 ± 0.1167	1.02 ± 0.1344	0.7389
Thalamus	0.70 ± 0.0376	1.04 ± 0.1078	0.7556
Hypothalamus	1.40 ± 0.1751	2.32 ± 0.0164	0.0004
Striatum	0.98 ± 0.1259	1.74 ± 0.3162	0.0013
Pallidum	1.19 ± 0.1403	2.07 ± 0.4068	0.0001
Olfactory	1.57 ± 0.2795	2.21 ± 0.5166	0.0125
Corpus Call	0.66 ± 0.0616	1.06 ± 0.1007	0.3912
White Matter	0.85 ± 0.0942	1.21 ± 0.2344	0.5445
Ventricles	0.76 ± 0.1489	1.02 ± 0.1888	0.9193
Entire Atlas	0.84 ± 0.0854	1.40 ± 0.2250	0.0478

[^{64}Cu]Cu-c[R_4W_5]C 4 h			
Tissue	Vehicle	LPS	P value
Medulla	0.85 ± 0.3509	0.98 ± 0.2381	>0.9999
Cerebellum	0.61 ± 0.1526	0.93 ± 0.0764	0.6146
Midbrain	0.44 ± 0.0613	0.69 ± 0.0936	0.9003
Pons	0.90 ± 0.4364	1.13 ± 0.2762	0.9572
Cortex	1.36 ± 0.1422	1.72 ± 0.3262	0.4365
Hippocampus	0.64 ± 0.0860	0.84 ± 0.1126	0.9885
Thalamus	0.46 ± 0.1028	0.57 ± 0.1568	>0.9999
Hypothalamus	1.18 ± 0.4057	1.34 ± 0.2991	0.9987
Striatum	1.15 ± 0.2427	1.42 ± 0.3495	0.8262
Pallidum	1.22 ± 0.3362	1.63 ± 0.3765	0.2459
Olfactory	1.73 ± 0.2030	2.13 ± 0.2000	0.274
Corpus Call	0.80 ± 0.1871	1.06 ± 0.2804	0.8945
White Matter	0.74 ± 0.1713	0.88 ± 0.1912	0.9997
Ventricles	0.62 ± 0.1991	0.78 ± 0.1760	0.9985
Entire Atlas	1.02 ± 0.1380	1.31 ± 0.1586	0.7897

[^{64}Cu]Cu-c[R_4W_5]C 8 h			
Tissue	Vehicle	LPS	P value
Medulla	0.84 ± 0.2166	0.68 ± 0.4077	>0.9999
Cerebellum	0.48 ± 0.1086	0.58 ± 0.3103	>0.9999
Midbrain	0.34 ± 0.0807	0.47 ± 0.2217	>0.9999
Pons	0.74 ± 0.1597	0.74 ± 0.4566	>0.9999
Cortex	0.93 ± 0.1353	1.02 ± 0.6332	>0.9999
Hippocampus	0.44 ± 0.0803	0.51 ± 0.2429	>0.9999
Thalamus	0.36 ± 0.0631	0.36 ± 0.1825	>0.9999
Hypothalamus	0.92 ± 0.0953	0.90 ± 0.4926	>0.9999
Striatum	0.84 ± 0.0735	0.79 ± 0.4829	>0.9999
Pallidum	0.97 ± 0.1147	0.92 ± 0.5532	>0.9999
Olfactory	1.24 ± 0.0785	1.24 ± 0.7622	>0.9999
Corpus Call	0.55 ± 0.1355	0.62 ± 0.4047	>0.9999
White Matter	0.58 ± 0.0740	0.54 ± 0.3092	>0.9999
Ventricles	0.46 ± 0.1284	0.43 ± 0.2564	>0.9999
Entire Atlas	0.75 ± 0.0673	0.79 ± 0.4478	>0.9999

[^{64}Cu]Cu-c[R_4W_5]C 12 h			
Tissue	Vehicle	LPS	P value
Medulla	0.97 ± 0.5238	0.99 ± 0.4925	>0.9999
Cerebellum	0.46 ± 0.1955	0.63 ± 0.0371	0.9998
Midbrain	0.43 ± 0.1039	0.57 ± 0.1393	>0.9999
Pons	0.91 ± 0.4497	0.90 ± 0.1958	>0.9999
Cortex	0.99 ± 0.1672	1.41 ± 0.4427	0.5378
Hippocampus	0.49 ± 0.1035	0.75 ± 0.1821	0.9762
Thalamus	0.44 ± 0.0829	0.67 ± 0.2511	0.9917
Hypothalamus	1.04 ± 0.2369	1.36 ± 0.4835	0.88
Striatum	0.99 ± 0.0891	1.31 ± 0.4217	0.8977
Pallidum	1.08 ± 0.1151	1.45 ± 0.4605	0.7245
Olfactory	1.38 ± 0.1291	1.70 ± 0.3253	0.8813
Corpus Call	0.61 ± 0.1808	1.01 ± 0.4529	0.6014
White Matter	0.66 ± 0.0717	0.92 ± 0.2861	0.9766
Ventricles	0.51 ± 0.1010	0.82 ± 0.2696	0.9111
Entire Atlas	0.83 ± 0.1128	1.11 ± 0.2655	0.9552

B.

Region	4 h	8 h	12 h
Medulla	0.0231	0.0237	0.3240
Cerebellum	0.0003	0.1891	0.0023
Midbrain	0.1038	0.1752	0.0176
Pons	0.1739	0.1498	0.1193
Cortex	0.2731	0.4181	0.8739
Hippocampus	0.0081	0.1195	0.1087
Thalamus	0.0329	0.0484	0.1546
Hypothalamus	0.1370	0.0530	0.0776
Striatum	0.5405	0.0577	0.2232
Pallidum	0.7454	0.0537	0.1572
Olfactory	0.3284	0.3285	0.2250
Corpus Call	0.5453	0.3013	0.8729
White Matter	0.0457	0.0680	0.2441
Ventricles	0.1240	0.0616	0.3451
Entire Atlas	0.1217	0.1720	0.2305

‡**Supplemental Table 7**. A. PET quantitation of [^{64}Cu]Cu-c[R_4W_5C] and [^{64}Cu]Cu-c[E_4W_5C] of select peripheral regions at 4, 8, and 12 h post-LPS injection. Data is represented as average %ID/g ± SD with *n* = 4 animals/group. P values comparing LPS groups of [^{64}Cu]Cu-c[E_4W_5C] vs. LPS of [^{64}Cu]Cu-c[R_4W_5C].

A.

[^{64}Cu]Cu-c[E_4W_5C]

12 h			
Tissue	Vehicle	LPS	P value
Liver	8.09 ± 0.86	20.10 ± 1.54	4.28E-05
SI	6.15 ± 0.73	10.01 ± 1.80	0.01071
Kidneys	6.50 ± 1.03	14.72 ± 1.45	0.000306
Lungs	3.35 ± 0.53	4.60 ± 0.41	0.020156

8 h			
Tissue	Vehicle	LPS	P value
Liver	9.38 ± 0.86	18.97 ± 1.78	0.000207
SI	8.02 ± 1.13	13.80 ± 2.38	0.007492
Kidneys	9.35 ± 1.19	13.33 ± 2.94	0.053726
Lungs	3.12 ± 0.50	4.50 ± 0.64	0.023478

4 h			
Tissue	Vehicle	LPS	P value
Liver	7.80 ± 1.59	15.55 ± 1.79	0.001754
SI	3.06 ± 0.96	4.77 ± 0.09	0.036791
Kidneys	11.96 ± 5.01	18.52 ± 2.14	0.090854
Lungs	4.42 ± 0.84	6.18 ± 0.68	0.032067

[^{64}Cu]Cu-c[R_4W_5C]

12 h			
Tissue	Vehicle	LPS	P value
Liver	17.85 ± 0.86	22.24 ± 2.81	0.060934
SI	3.81 ± 0.79	4.21 ± 0.14	0.433827
Kidneys	5.96 ± 2.24	8.01 ± 2.24	0.285222
Lungs	2.30 ± 1.11	3.28 ± 1.09	0.297125

8 h			
Tissue	Vehicle	LPS	P value
Liver	18.94 ± 3.42	16.04 ± 8.48	0.549311
SI	3.48 ± 0.68	2.76 ± 0.82	0.225002
Kidneys	5.78 ± 1.37	8.34 ± 3.25	0.197844
Lungs	1.96 ± 0.59	2.78 ± 0.70	0.122158

4 h			
Tissue	Vehicle	LPS	P value
Liver	17.85 ± 1.80	18.42 ± 2.79	0.745327
SI	3.43 ± 0.78	3.38 ± 1.01	0.936461
Kidneys	10.44 ± 1.17	8.55 ± 2.60	0.234361
Lungs	3.04 ± 1.24	3.96 ± 0.73	0.247581

B.

12 h	
Tissue	P value
Liver	0.311215
SI	0.01219
Kidneys	0.120675
Lungs	0.005155

8 h	
Tissue	P value
Liver	0.589591
SI	0.091147
Kidneys	0.020825
Lungs	0.000309

4 h	
Tissue	P value
Liver	0.333823
SI	0.009154
Kidneys	0.027715
Lungs	0.144527

‡**Supplemental Table 8**. A. Full ex vivo biodistribution of [^{64}Cu]Cu-c[R_4W_5C] and [^{64}Cu]Cu-c[E_4W_5C] with respective P values (as determined by unpaired two-tailed t-test) comparing vehicle and LPS-treated groups at 24 h-post LPS administration. Data is represented as average %ID/g ± SD (*n* = 4/group for vehicle, *n* = 2/LPS for group). P values comparing LPS groups of [^{64}Cu]Cu-c[E_4W_5C] vs. LPS of [^{64}Cu]Cu-c[R_4W_5C].

A.

[^{64}Cu]Cu-c[E_4W_5C]				[^{64}Cu]Cu-c[R_4W_5C]			
Tissue	Vehicle	LPS	P value	Tissue	Vehicle	LPS	P value
Blood	0.98 ± 0.18	2.58 ± 1.28	0.0231	Blood	0.94 ± 0.08	1.18 ± 0.31	0.2357
Heart	2.01 ± 0.35	2.23 ± 0.97	0.6473	Heart	1.21 ± 0.10	0.99 ± 0.32	0.2778
Lungs	1.76 ± 0.93	3.70 ± 0.30	0.0402	Lungs	1.63 ± 0.80	1.45 ± 1.30	0.8131
Liver	8.22 ± 1.27	20.98 ± 9.22	0.0161	Liver	18.54 ± 4.58	20.57 ± 12.23	0.7457
Spleen	1.17 ± 0.27	1.58 ± 0.85	0.3258	Spleen	5.25 ± 0.57	5.59 ± 3.51	0.8305
Pancreas	1.00 ± 0.25	1.99 ± 1.30	0.1157	Pancreas	1.18 ± 0.28	1.41 ± 0.66	0.5319
Stomach	2.10 ± 0.55	1.77 ± 1.00	0.5761	Stomach	1.82 ± 1.37	0.82 ± 0.53	0.3487
SI	2.64 ± 0.56	10.74 ± 5.54	0.0123	SI	2.97 ± 0.14	5.16 ± 4.18	0.3340
LI	4.68 ± 0.95	2.20 ± 1.42	0.0379	LI	3.10 ± 0.77	1.69 ± 0.70	0.1630
Kidneys	4.53 ± 1.05	8.47 ± 2.32	0.0200	Kidneys	3.47 ± 0.20	5.36 ± 1.29	0.1333
Muscle	0.44 ± 0.13	0.70 ± 0.43	0.2243	Muscle	0.35 ± 0.08	0.34 ± 0.14	0.9149
Bone	0.90 ± 0.26	1.22 ± 0.57	0.3597	Bone	1.27 ± 0.60	1.27 ± 0.52	0.9857
Skin	0.42 ± 0.06	0.95 ± 0.12	0.0004	Skin	0.76 ± 0.28	0.52 ± 0.02	0.2911
Brain	0.34 ± 0.06	0.48 ± 0.01	0.0264	Brain	0.12 ± 0.02	0.09 ± 0.01	0.2129

B.

Tissue	P value
Blood	0.271416
Heart	0.229126
Lungs	0.138901
Liver	0.973091
Spleen	0.257107
Pancreas	0.631845
Stomach	0.358247
SI	0.373264
LI	0.693616
Kidneys	0.238848
Muscle	0.379655
Bone	0.939168
Skin	0.041169
Brain	0.000693

REFERENCES

1. Shen C, Menon R, Das D, Bansal N, Guduru N, Jaegle S, Reshetnyak Y. K. The protein fluorescence and structural toolkit: Database and programs for the analysis of protein fluorescence and structural data. Proteins. 2008;71(4):1744-54.
2. Dierckx RA, de Wiele CV. FDG uptake, a surrogate of tumour hypoxia? Eur J Nuc Med and Mol Imag. 2008;35(8), 1544-1549.
3. Longo DL, Bartoli A, Consolino L, Bardini P, Arena F, Schwaiger M, Aime S. In Vivo Imaging of Tumor Metabolism and Acidosis by Combining PET and MRI-CEST pH Imaging. Cancer Res. 2016;76(22):6463-6470.
4. Hoiland, RL, Bain, AR, Rieger, MG, Bailey,2 DM, Ainslie, PN. Hypoxemia, oxygen content, and the regulation of cerebral blood flow. Am J Physiol Regul Comp Physiol. 2016;310(5): R398-R413.
5. Michael T. Alkire, MT, Pomfrett, CJD, Haier, RJ, Gianzero, MV, Chan, CM, Jacobsen, BP, Fallon JH. Functional Brain Imaging during Anesthesia in Humans: Effects of Halothane on Global and Regional Cerebral Glucose Metabolism. Clin Sci. 1999;90(3): 701-709.
6. Alstrup, AKO, Landau, AM, Holden, JE, Jakobsen S, Schacht, AC, Audrain, H, Wegener G, Hansen AK, Gjedde, A, Doudet, DJ. Effects of Anesthesia and Species on the Uptake or Binding of Radioligands In Vivo in the Göttingen Minipig. Biomed Res Int. 2013; 2013: 808713.